Amoeboid Swimming: A Generic Self-Propulsion of Cells in Fluids by Means of Membrane Deformations

Alexander Farutin,[1,*] Salima Rafaï,[1] Dag Kristian Dysthe,[2] Alain Duperray,[3] Philippe Peyla,[1] and Chaouqi Misbah[1,†]

[1]*Laboratory of Interdisciplinary Physics, UMR 5588, Université Joseph Fourier and CNRS, F-38041 Grenoble, France*

[2]*Physics of Geological Processes, University of Oslo, P.O. Box 1048 Blindern, N-0316 Oslo, Norway*

[3]*Centre de Recherche INSERM U823 Institut Albert Bonniot, BP170 38042 Grenoble Cedex 9, France*

(Received 23 July 2013; published 26 November 2013)

Microorganisms, such as bacteria, algae, or spermatozoa, are able to propel themselves forward thanks to flagella or cilia activity. By contrast, other organisms employ pronounced changes of the membrane shape to achieve propulsion, a prototypical example being the *Eutreptiella gymnastica*. Cells of the immune system as well as *dictyostelium* amoebas, traditionally believed to crawl on a substratum, can also swim in a similar way. We develop a model for these organisms: the swimmer is mimicked by a closed incompressible membrane with force density distribution (with zero total force and torque). It is shown that fast propulsion can be achieved with adequate shape adaptations. This swimming is found to consist of an entangled pusher-puller state. The autopropulsion distance over one cycle is a universal linear function of a simple geometrical dimensionless quantity $A/V^{2/3}$ (V and A are the cell volume and its membrane area). This study captures the peculiar motion of *Eutreptiella gymnastica* with simple force distribution.

DOI: 10.1103/PhysRevLett.111.228102 PACS numbers: 47.63.Gd, 47.15.G−, 47.61.−k

Introduction.—In nature, organisms that can propel themselves in a fluid medium are ubiquitous. While larger organisms, such as fish, use inertia in their motion, some microorganisms move at low Reynolds number (Re), where viscous forces dominate inertial effects: they are classified as microswimmers [1,2]. Among them, a lot of microorganisms [3,4], like spermatozoa [5], bacteria [6], or microalgae [7,8], can move with the help of flagella or cilia [6,9], and recently several publications have been dedicated to them in order to understand the complex coupling between their motion and the hydrodynamics of the surrounding fluid.

However, some other organisms, like *Eutreptiella gymnastica* [10] (a common representative of euglenids of marine phytoplankton) use both flagella and pronounced shape changes to swim. While the conventional mode for amoeboid locomotion is crawling on solid surfaces, it was shown recently [11,12] that *dictyostelium* amoebas are also able to swim by deforming their bodies with a process similar to the one they use for crawling. Indeed, they can swim with speeds similar to those on a solid substrate. A similar behavior [11] is observed for neutrophils, i.e., the white blood cells in mammals that form an essential part of the innate immune system.

This peculiar self-propulsion with shape deformations requires the movement of the cell's surface to occur from the cell's front toward its rear, and this deformation moves back and forth along the swimming direction. Because of Purcell's theorem [1], this motion at low Re must break the reciprocal time symmetry.

Theoretical studies of self-propulsion with shape deformations have been considered for ellipsoidal particles [13,14] and general strokes [15–18] or shapes [19] optimizing the dissipation. The physics of a cell membrane incompressibility adopted here (verified for *eutreptiella* [20]) will be seen to have a strong impact on swimming. On the one hand, local inextensibility of the cell membrane is a constraint that is known to induce a variety of dynamical motions (like within a red blood cell) [21] which are absent for droplets. On the other hand, membrane incompressibility limits membrane protrusions in the motility process [11,12]. This is reflected on the propulsion law, as we shall see.

We propose an elementary model describing the self-propulsion of a cell due to shape deformation of its inextensible membrane. We first consider a quasispherical swimmer for which an explicit analytical solution can be obtained. We then explore large swimmer deformations by means of numerical simulations. This minimal model captures several swimming features. We make predictions that are not devoid of experimental testability.

The model.—The swimmer has an inextensible fluid membrane encapsulating a Newtonian fluid with viscosity $\lambda\eta$ and floating in fluid of viscosity η (λ is the viscosity contrast). The swimmer is capable of changing its shape by applying active forces from its membrane. We restrict the model to normal active forces in order to remain within a minimal model, although tangential active forces can be accounted for in principle. Because of inextensibility, the membrane exerts passive tension forces on the surrounding liquids in reaction to active forces. We assume that there is no exchange of matter between the interior and exterior of the swimmer on the relevant time scales, as well as no-slip boundary conditions at the membrane. Finally, the

swimmer is considered as neutrally buoyant so that the total force and torque exerted by the swimmer on the liquids vanish at each time. Our model can be viewed in a first step applicable to artificial swimmers made of vesicles or red blood cells. This work should serve as a basis for more refined studies relevant to complex biological cells.

Under these conditions, the state of a microswimmer is fully described by its shape and position, and the only conserved geometrical properties are the volume V and the surface area A (analysis of some specimens of euglenid swimming supports these assumptions [20]).

Let r_v be the radius of the equivalent sphere, such that $V = 4\pi r_v^3/3$. The deflation from the sphere is specified by the normed excess area Γ, $A = 4\pi r_v^2(1+\Gamma)$ ($\Gamma = 0$ for a sphere).

Analytical results can be obtained for an almost-spherical swimmer ($\Gamma \ll 1$). The deviation from a sphere ($r = r_v$) of the shape of the swimmer is parametrized (in the comoving frame) by the scalar function

$$\rho(\boldsymbol{x}) = \sum_{l=0}^{l_{\max}} \sum_{m=-l}^{l} \rho_{l,m} Y_{l,m}(\boldsymbol{x}), \tag{1}$$

where $Y_{l,m}$ are spherical harmonics, $\boldsymbol{x} \equiv \boldsymbol{r}/r$, $\boldsymbol{r}$ represents swimmer membrane vector position, and $\rho_{l,m}$ are time-dependent amplitudes (to be determined). $l_{\max}$ specifies the maximum number of harmonics. We have checked that using harmonics of order higher than 6 does not result in a noticeable increase of traveled distance during one stroke cycle.

Likewise, the amplitude of the active forces $F(\boldsymbol{x})$ exerted by the swimmer on the fluid is decomposed as in Eq. (1) with amplitudes $F_{l,m}$. To enforce local membrane incompressibility, a Lagrange multiplier $\zeta(\boldsymbol{x})$ is introduced, which acts as a position-dependent surface tension. The corresponding force takes the form (see Ref. [22])

$$\boldsymbol{F}^{\text{tens}}(\boldsymbol{x}) = -H(\boldsymbol{x})\zeta(\boldsymbol{x})\boldsymbol{n}(\boldsymbol{x}) + \boldsymbol{\nabla}^s\zeta(\boldsymbol{x}), \tag{2}$$

where $H(\boldsymbol{x})$ is the mean curvature, $\boldsymbol{n}(\boldsymbol{x})$ is the outward normal to the membrane, and $\boldsymbol{\nabla}^s = [\boldsymbol{I} - \boldsymbol{n}(\boldsymbol{x}) \otimes \boldsymbol{n}(\boldsymbol{x})].\boldsymbol{\nabla}$ is the surface gradient operator on the membrane. The local incompressibility of the membrane demands that the velocity field $\boldsymbol{v}(\boldsymbol{x})$ have zero surface divergence at any point of the membrane.

The total force $\boldsymbol{F}^{\text{tot}}$ is a sum of active and passive forces:

$$\boldsymbol{F}^{\text{tot}}(\boldsymbol{x}) = F(\boldsymbol{x})\boldsymbol{n}(\boldsymbol{x}) + \boldsymbol{F}^{\text{tens}}(\boldsymbol{x}). \tag{3}$$

The Stokes equations for internal and external fluids can be solved following a procedure outlined, e.g., in Ref. [23]. Some technical details can be found in Ref. [22], while here we merely focus on the outcome.

The results: Axisymmetric swimming.—This configuration is sufficient to expose the main results. Only harmonics with $m = 0$ survive (below, the subscript "m" is omitted, i.e., $\rho_{l,0} \equiv \rho_l$ and $F_{l,0} \equiv F_l$). To the leading order, the evolution of the shape of the swimmer obeys [22]

$$\dot{\rho}_l(t) = \beta_l\left[F_l(t) - \frac{\zeta_0(t)}{r_v}\alpha_l\rho_l(t)\right], \qquad l > 1, \tag{4}$$

where t is the time, $\dot{\rho}_l(t) = d\rho_l(t)/dt$, and the swimming velocity $\boldsymbol{v}^c$ is found to be given by

$$\boldsymbol{v}^c = \dot{\boldsymbol{r}}^c(t) = r_v \sum_{l=2}^{l_{\max}-1} [\mu_l\rho_{l+1}(t)\dot{\rho}_l(t) - \nu_l\rho_l(t)\dot{\rho}_{l+1}(t)]. \tag{5}$$

The coefficients α_l, β_l, μ_l, and ν_l depend on l and viscosity contrast λ and are listed in Ref. [22].

The isotropic part of the Lagrange multiplier ζ_0 is calculated by substituting Eq. (4) into the time derivative of the fixed surface area condition yielding

$$\sum_{l=2}^{l_{\max}} \frac{\alpha_l\rho_l^2}{2(2l+1)} = \Gamma. \tag{6}$$

ζ_0 is a nonlinear function of ρ_l [22] so that Eq. (4) is nonlinear in ρ (its explicit form is listed in Ref. [22]). This markedly differs from studies not imposing incompressibility where the evolution equations are linear [15]. Results (4) and (5) are our basic equations.

Swimming pattern.—In order to mimic the swimming strategies of actual living organisms, we allow for a rather restricted set of swimming patterns: we assume that the swimming can be represented as a series of elementary strokes, the intervals of time, during which the distribution of active normal forces $F(\boldsymbol{x})$ does not vary. If the amplitudes F_l are constant in time, the solution of Eq. (4) relaxes to a steady-state value, the time derivatives $\dot{\rho}_l$ decrease to zero exponentially, and the swimmer stops moving according to Eq. (5). It must then change the distribution of normal active forces, thus starting a new elementary stroke. In this study, we consider full elementary strokes, i.e., the strokes that last until the shape reaches saturation and the propulsion stops. The distance traveled during one full elementary stroke does not change if all force amplitudes F_l are multiplied by the same number. Indeed, multiplying F_l and $\zeta_0(t)$ by a constant a and dividing the time t by a leaves Eqs. (4)–(6) invariant. In other words, if the amplitude of active forces is doubled, the shape of the swimmer reaches the saturation twice faster, so that despite the fact that at the beginning of the stroke the velocity is doubled, it falls to zero twice faster, and the traveled distance remains unchanged. Thus, the distance during an elementary stroke is unambiguously defined by the shape of the swimmer at the beginning and at the end of the stroke.

Swimming strategy among a large manifold of possibilities.—Consider a stroke cycle, a sequence of full elementary strokes that returns the swimmer to its initial shape. If the swimmer exhibits a finite displacement during one stroke cycle, it can swim any distance by duplicating the strokes. The swimming velocity is equal to the

displacement during one stroke cycle times the frequency of the stroke cycles. One could ask then, "What would be the fastest way to swim?" That is, which distributions of active normal forces during elementary strokes should the swimmer deploy in order to achieve the maximal displacement during one stroke cycle?

For analytical tractability, we set $l_{\max} = 3$. This entails that only ρ_2 and ρ_3 are nonzero [see Eq. (4)] but are linked by constraint (6), leaving us with only one degree of freedom. Interestingly enough, swimming can occur despite a single degree of freedom; this does not contradict the scallop theorem, as shown below. The constraint (6) describes an ellipse in the (ρ_2, ρ_3) plane. The simplest nontrivial cycle of shape changes corresponds to a complete turn around the ellipse. The displacement after one cycle is obtained by time integration of Eq. (5):

$$\Delta r_z^c = \int_0^T \dot{r}_z^c dt = \int_0^T [\mu_2 \rho_3(t)\dot{\rho}_2(t) - \nu_2 \rho_2(t)\dot{\rho}_3(t)]dt$$
$$= \oint \mu_2 \rho_3 d\rho_2 - \nu_2 \rho_2 d\rho_3 = (\mu_2 + \nu_2) \int d\rho_2 d\rho_3, \quad (7)$$

where T is the length of the stroke cycle. The last integral in Eq. (7) is the area of the ellipse. From the equation of the ellipse (6) the area is determined and Eq. (7) yields (by using expressions of μ_l and ν_l given in Ref. [22])

$$\Delta r_z^c = \frac{3\pi\Gamma}{\sqrt{14}} r_v \simeq 2.5\Gamma r_v. \quad (8)$$

This result is independent of the force distribution (as well as of their temporal evolution) or any other parameter but involves only a universal constant and geometrical quantities. If higher harmonics are taken into account ($l_{\max} > 3$), however, there exists a large manifold of swimming patterns. The question naturally arises about the selection of swimming pattern. Previous studies used dissipation [15–19] as a criterion for selection. Here we optimize the swimming speed instead. We propose that the elementary strokes can only be performed at a finite rate due to the time required for the adaptation of the internal biochemical machinery of the cell. Therefore, we choose to maximize the distance traveled during one stroke cycle while keeping the number of elementary strokes per cycle fixed. In order to find the optimal swimming strategy in this sense, we fix the number of elementary strokes during one cycle and solve for optimal distributions of normal forces F_l during each elementary stroke by numerical maximization of Δr_z^c. We have checked that the maximum displacement during a three-stroke cycle is not too much affected upon increasing the number of spherical harmonics $l_{\max}$: for $l_{\max} = 4$, $\Delta r_{\max}^c / r_v = 3.10\Gamma$, for $l_{\max} = 6$ or $l_{\max} = 16$, $\Delta r_{\max}^c / r_v = 3.24\Gamma$. The fastest three-stroke cycle for $l_{\max} = 16$ and $\lambda = 1$ is shown in Fig. 1(a). A striking feature of this snapshot is the absence of cusps or high-wave-vector wrinkles observed in optimal strokes of swimmers with extensible membrane [15–18].

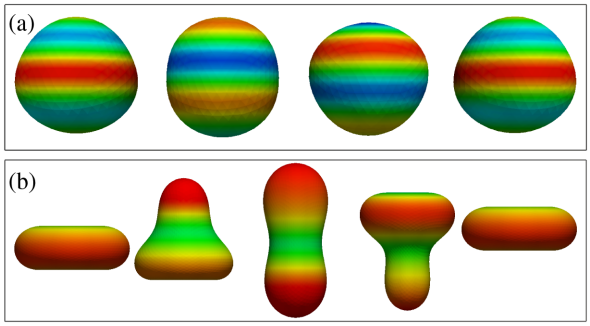

FIG. 1 (color online). (a) Shape transformation during a three-stroke cycle for fastest swimming. $l_{\max} = 16$. The normed excess area $\Gamma = 0.025$. Color code shows the distribution of active forces necessary to go to the next shape. (b) Large deformation swimmer with $\Gamma = 0.16$. Colors of the insets correspond to $F(x)$ (red outward, blue inward directed force).

We attribute this difference to the effect of membrane inextensibility.

Pusher or puller?—So far, two main distinct swimmers have been identified in the literature: pusher and puller [2,24]. It is thus natural to ask whether or not the present swimmer belongs to any of these two categories. The four strokes of the cycle are identified as follows (Fig. 2): (i) oblatelike shape (bottom left Fig. 2) with ($\rho_2 < 0$, $\rho_3 = 0$) showing flow lines in the swimming direction pointing along the swimming direction, (ii) forward-pointed stage ($\rho_2 = 0$, $\rho_3 > 0$) (bottom right), where flow lines point outward along the swimming direction (typical for pushers), (iii) prolatelike stage ($\rho_2 > 0$, $\rho_3 = 0$)

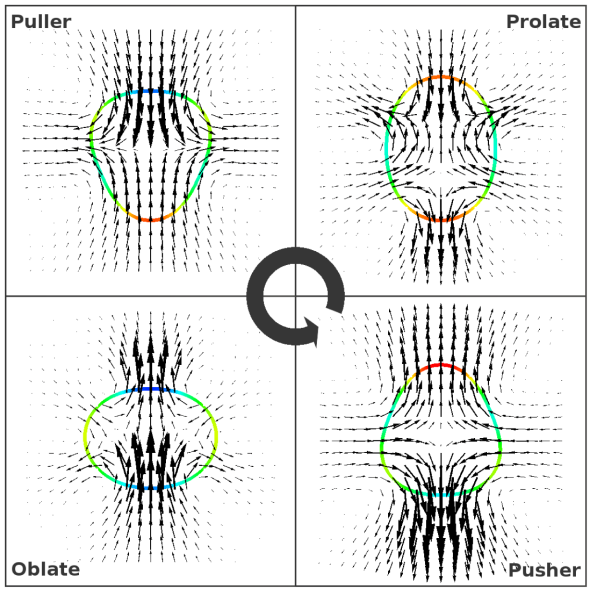

FIG. 2 (color online). Numerical simulations of flow around a swimmer. Time flow is counterclockwise. Symmetry axis of the swimmer is vertical. Color code shows the intensity of the active force F. Swimming direction points towards the top of the page. $\Gamma = 0.0134$.

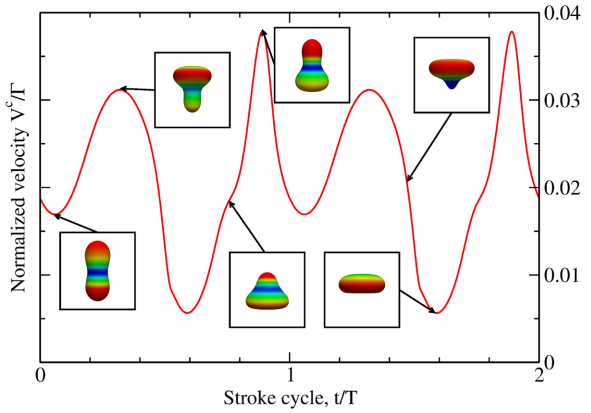

FIG. 3 (color online). Swimming velocity as a function of time. $r_0 = \eta = \lambda = 1$. The insets show the instantaneous shapes of the swimmer. Colors of the insets correspond to $F(x)$ (red outward, blue inward directed force).

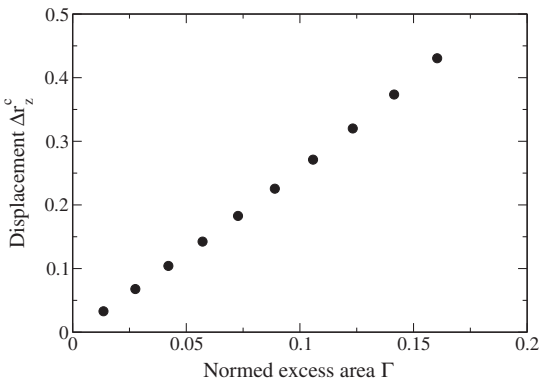

FIG. 4. Swimming propulsion distance over one cycle as a function of excess area Γ.

(top right), with flow lines in the swimming direction pointing against swimming, and (iv) a backward-pointed stage ($\rho_2 = 0$, $\rho_3 < 0$) where flow lines point inward along the swimming direction (typical for pullers). Overall, within a cycle of swimming, pulling and pushing coexist in a complex entangled state; thus, the denomination entangled pusher puller is adopted. It is found that the puller and pusher phases perfectly cancel each other (time-average swimmer stresslet is exactly zero) in the small deformation regime and when $l_{\max} = 3$. This ceases to be the case in general if $l_{\max} > 3$.

Strong shape deformation.—Real cells like *Eutreptiella gymnastica* or neutrophils undergo ample shape deformation. In order to dispose of a quantitative information, we have performed a full numerical simulation accounting for large deformations by means of 3D boundary integral formulation. This is a formidable task even for passive particles (like red blood cells under flow) resolved only recently [25]. We set $\Gamma = 0.16$. and apply active forces specified by two nonzero amplitudes (for illustration)

$$F_2 = 2\cos(\omega t), \qquad F_3 = -2\sin(\omega t). \tag{9}$$

Despite this form, higher harmonics are excited in the shape of the swimmer. The swimming frequency is set to $\omega = 0.05$ (the swimmer has sufficient time to adapt to the distribution of active forces). Swimming snapshots are shown in Fig. 1(b) resembling those of *Eutreptiella gymnastica*. Figure 3 shows the instantaneous velocity. We found for the simulation reported in Fig. 1 that on average the swimmer behaves as a puller.

A systematic numerical analysis for various values of Γ for a given force distribution is performed. Interestingly enough, the propulsion distance over one swimming cycle follows almost a linear relationship with Γ,

$$\frac{\Delta r_z^c}{r_v} \sim c\Gamma, \qquad c \simeq 2.4\text{–}2.7. \tag{10}$$

The prefactor is close to that in Eq. (8). The results are reported in Fig. 4. Result (10) can be understood from a heuristic argument. The active force F creates a viscous tension, $F \sim \eta V/R_A$, where R_A is a typical length scale of the cell protrusion of order of $\sqrt{\Gamma}$. The time scale for a stroke is given (from dimensional analysis) by $\tau \sim (\eta/F)a$, where a is a dimensionless quantity defining how fast the shape achieves saturation. The more there is excess area, the longest is τ, and from the shape equation, we have to leading order $a \sim \sqrt{\Gamma}$ (see Ref. [22]), so that the propulsion distance is $V\tau \sim \Gamma$. The law (10) is not devoid of experimental testability. For *Eutreptiella gymnastica* with size of order 20 μm, with $\tau \sim 10$ s, we find a force of order 10 pN. The reduced area Γ is of about 0.2 [20], and using Eq. (10), we find $(\Delta r_z^c/r_v) \sim 0.4$ and a speed of propulsion (by using the stroke frequency) of about 1 μm/s. These are consistent with known data [20].

In conclusion, the peculiar motion of *eutreptiella* is recovered with a simple distribution of normal forces, and the propulsion distance is obtained in terms of geometrical quantities. Some euglenids change volume during swimming [20], whereas several animal cells seem to change area during spreading on substrate [26] (the situation during swimming is unclear). It is hoped to investigate this matter in a future work.

We acknowledge fruitful discussion with Karin John. A. F. and C. M. gratefully acknowledge financial support from CNES and ESA. S. R. and P. P. are supported by ANR, project MICMACSWIM. D. K. D. thanks the EU (European Union) for financial support during his stay in France.

*alexandr.farutin@ujf-grenoble.fr
†chaouqi.misbah@ujf-grenoble.fr

[1] E. M. Purcell, Am. J. Phys. **45**, 3 (1977).
[2] E. Lauga and T. Powers, Rep. Prog. Phys. **72**, 096601 (2009).
[3] M. L. Ginger, N. Portman, and P. G. McKean, Nat. Rev. Microbiol. **6**, 838 (2008).

[4] K. F. Jarrell and M. J. McBride, Nat. Rev. Microbiol. **6**, 466 (2008).
[5] J. Gray and G. Hancock, J. Exp. Biol. **32**, 802 (1955).
[6] H. C. Berg, *E. coli in Motion* (Springer, New York, 2004).
[7] T. Ishikawa and T. Pedley, J. Fluid Mech. **588**, 437 (2007).
[8] M. Garcia, S. Berti, P. Peyla, and S. Rafai, Phys. Rev. E **83**, 035301 (2011).
[9] L. Turner, W. Ryu, and H. Berg, J. Bacteriol. **182**, 2793 (2000).
[10] J. Throndsen, Norwegian Journal of botany **16**, 161 (1969).
[11] N. P. Barry and M. S. Bretscher, Proc. Natl. Acad. Sci. U.S.A. **107**, 11 376 (2010).
[12] A. J. Baea and E. Bodenschatz, Proc. Natl. Acad. Sci. U.S.A. **107**, E165 (2010).
[13] T. Ohta and T. Ohkuma, Phys. Rev. Lett. **102**, 154101 (2009).
[14] T. Hiraiwa, K. Shitaraa, and T. Ohta, Soft Matter **7**, 3083 (2011).
[15] A. Shapere and F. Wilczek, Phys. Rev. Lett. **58**, 2051 (1987).
[16] J. E. Avron, O. Gat, and O. Kenneth, Phys. Rev. Lett. **93**, 186001 (2004).
[17] F. Alouges, A. Desimone, and L. Heltai, Math. Models Methods Appl. Sci. **21**, 361 (2011).
[18] J. Lohéac, J.-F. Scheid, and M. Tucsnak, Acta Appl. Math. **123**, 175 (2013).
[19] A. Vilfan, Phys. Rev. Lett. **109**, 128105 (2012).
[20] M. Arroyo, L. Heltai, D. Millán, and A. DeSimone, Proc. Natl. Acad. Sci. U.S.A. **109**, 17 874 (2012).
[21] A. Z. K. Yazdani and P. Bagchi, Phys. Rev. E **84**, 026314 (2011).
[22] See Supplemental Material at http://link.aps.org/supplemental/10.1103/PhysRevLett.111.228102 for a movie of the swimming motion, details of the analytical and numerical methods, coefficients of the governing equations, derivation of the tension force and the scaling analysis of the problem.
[23] G. Danker, T. Biben, T. Podgorski, C. Verdier, and C. Misbah, Phys. Rev. E **76**, 041905 (2007).
[24] D. Saintillain and M. Shelley, C.R. Phys. **14**, 497 (2013).
[25] A. Farutin and C. Misbah, Phys. Rev. Lett. **109**, 248106 (2012).
[26] M. Sheetz, J. Sable, and H. Dobereiner, Annu. Rev. Biophys. Biomol. Struct. **35**, 417 (2006).